Optimization-based estimation of power capacity profiles for activity-based residential loads

Citation for published version:
Gomez-herrera, JA & Anjos, MF 2019, 'Optimization-based estimation of power capacity profiles for activity-based residential loads', *International Journal of Electrical Power & Energy Systems*, vol. 104, pp. 664-672. https://doi.org/10.1016/j.ijepes.2018.07.023

Digital Object Identifier (DOI):
10.1016/j.ijepes.2018.07.023

Link:
Link to publication record in Edinburgh Research Explorer

Document Version:
Peer reviewed version

Published In:
International Journal of Electrical Power & Energy Systems

Optimization-Based Estimation of Power Capacity Profiles for Activity-Based Residential Loads

Juan A. Gomez-Herrera[a,*], Miguel F. Anjos[a]

[a] GERAD and Department of Mathematics and Industrial Engineering, Polytechnique Montreal, C.P. 6079, Succ. Centre-Ville, Montreal, QC, Canada H3C 3A7

Abstract

This paper proposes a framework to determine capacity profiles in smart buildings. In this scheme the users choose a level of power capacity to account for their stochastic demand while paying the corresponding electricity prices through a flexible time-and-level-of-use pricing policy. We formulate a two-stage stochastic optimization model that minimizes the total cost of booking a power capacity level and meeting the energy demand for the planning horizon. We present two approaches to select the scenarios for the stochastic optimization. In the first approach, we assume that the probability distributions of the start times of the loads are known, and the scenarios are generated using those distributions. In the second approach, we assume that only historical consumption data is available and we propose a new algorithm to build the scenarios using this data. Our simulation experiments validate the performance of both approaches and report cost savings of up to 16%.

Keywords: Smart buildings, power demand, residential load sector, user behavior, activity-based loads, stochastic optimization.

1. Notation

Sets

$t \in T$	Set of time frames in horizon.
$m \in M$	Set of loads.
$i \in S$	Set of scenarios.
$j \in Q^L$	Set of intervals of the cost step function for the lower tariff.
$q \in Q^H$	Set of intervals of the cost step function for the higher tariff.

Optimization Parameters

K_t^0	Time of use tariff in time frame t (¢/kWh).
K_{jt}^L	Lower tariff in interval j in time frame t (¢/kWh).
K_{qt}^H	Higher tariff in interval q in time frame t (¢/kWh).
K_t^F	Booking cost in time frame t (¢/kWh).
C_{jt}^L	Capacity lower bound in interval j in time frame t for the lower tariff (kW).
C_{qt}^H	Capacity lower bound in interval q in time frame t for the higher tariff (kW).
π_{it}	Probability of scenario i in time frame t.
D_{it}	Demand for scenario i in time frame t.

Optimization Variables

x_{ijt}^L	Electricity consumption at lower tariff in scenario i, time frame t, and interval j (kWh).
x_{iqt}^H	Electricity consumption at higher tariff in scenario i, time frame t, and interval q (kWh).
c_{jt}	Booked capacity in time frame t and interval j (kW).
$\bar{c}_{qt}$	Auxiliary variable to identify the higher tariff interval q in time frame t.
ϕ_{jt}	$\begin{cases} 1 & \text{Capacity in time frame } t \text{ belongs to interval } j \text{ for the lower tariff} \\ 0 & \text{Otherwise} \end{cases}$
δ_{qt}	$\begin{cases} 1 & \text{Capacity in time frame } t \text{ belongs to interval } q \text{ for the higher tariff} \\ 0 & \text{Otherwise} \end{cases}$

Scenario Generation from Distributions (SfD)

P_m	Power consumption of load m (kW).
L_m	Duration of load m (h).
$\tilde{X}_{mt}$	$\begin{cases} 1 & \text{Load } m \text{ is active in time frame } t \\ 0 & \text{Otherwise} \end{cases}$
σ	Standard deviation for the loads arrival time.
ρ	Significance threshold for scenario elimination.

Scenario Generation from Historical Data (SfH)

N	Number of days in Γ.
$\Gamma \in \mathbb{R}^{N \times \lvert T \rvert}$	Historical load consumption.
G	Number of time segments.
$\bar{G}(n)$	Number of time segments in iteration n.
α	Number of iterations with a constant $\bar{G}(n)$.
β	Stopping criterion.

*Corresponding author

Email address: juan.gomez@polymtl.ca (Juan A. Gomez-Herrera)

2. Introduction

The increasing development of smart grids (SGs) creates potential benefits and challenges for utilities, consumers, and society in general. A SG allows information flow among all the participants [1], supporting decisions that ensure the stability, reliability, and economic viability of the system.

In this context, the consumers (end-users) can become decision-makers and participate in grid's decisions through demand response (DR) programs [2]. DR programs are designed to encourage end-users to change their consumption preferences in a way that is beneficial for the grid, normally in exchange for compensation.

DR programs can be classified in two groups: incentive-based programs and pricing programs. In incentive-based programs the consumer commits to reducing consumption over a determined period of time under prespecified conditions.

In pricing DR programs, the utility offers a variable tariff, expecting that the user will react by shifting load to cheaper time frames. If the users do not shift they pay more to meet their energy requirements. These pricing policies normally reflect the aggregated peak of demand and therefore the utility's generation costs. They are mostly oriented to customers in residential and commercial sectors and have particular potential in smart buildings [3], where the end-users can seek to benefit while meeting the grid requirements.

The residential and commercial sectors have specific characteristics that must be taken into account. First, the demand is driven by a large number of end-users with low individual consumption. Second, the consumption is triggered by the user behavior, which may be (highly) stochastic.

There are various models that consider user behavior. Some approaches seek to predict the future user consumption based on historical data. The review presented by [4] contains some of the most common bottom-up approaches to load forecasting. The model presented in [5] determines consumption profiles based on the aggregation of individual loads, the number of people in the housing unit, and their activity profiles. In a similar way, [6] uses a Markov-chain Monte-Carlo model to compute the activity profiles in order to estimate realistic load profiles for a wide variety of housing units. The approach presented in [7] uses logistic and Poisson regression to model the correlational and consistency elements of the shared activities of multiple inhabitants in a household. Poisson regression accounts for the activities that can occur multiple times during the day, and logistic regression estimates the probability for each event.

The characterization framework in [8] analyzes the controllable demand and its potential savings for users participating in an energy management system. Similarly, the approach in [9] estimates consumption profiles by fitting probability density distributions over a historical set for single and multiple housing units.

The importance of a consumption-aware user is discussed in [10]. This survey includes elements such as potential energy savings, activities with higher potential impact, and the availability of information and automation in the building.

Besides estimating load and understanding user behavior, there are various strategies for integrating the consumers into the grid decisions. The authors in [11] present a comprehensive review of optimization-based approaches for demand-side management (DSM). They compare the system granularity, the time scale and the type of demand (deterministic or stochastic). DSM normally deals with user's costs and demand satisfaction. In [12], [13], and [14], the user preferences are typically hard constraints and are met while optimizing the energy consumption or peak reduction.

In a similar way, the mixed integer linear optimization model in [15] minimizes the cost for the user in a day-ahead context. This approach considers priorities for the operation of a set of dispatchable appliances. The mixed integer nonlinear model in [16] maximizes the difference between a utility and a cost function while determining the operation time and the power consumption level of each device. On the other hand, multi-objective optimization is used to trade-off energy costs and comfort in [17] and [18].

As previously mentioned, user participation can be encouraged by DR pricing programs. A pricing policy that considers user behavior facilitates the user's integration into the SG decisions. Different pricing policies are assessed in [19] and [20] to explore the effect on user participation and grid performance. Declining block rates are analyzed in [21] to achieve a balance between electricity cost and user comfort. The role of electricity tariffs in solar panel penetration and the benefit for residential users are explored in [22]. In other cases there is a negotiation process. The user behavior is considered during the process of setting prices in [23]. In this case a bilevel optimization approach is used to find a trade-off between the revenue obtained by the energy provider and the user dissatisfaction.

In this article we propose a novel framework that integrates features of user behavior models, user participation through DSM, and DR pricing programs in order to provide residential and commercial users, and utilities with a tool to support decisions within a SG.

The proposed framework determines power capacity profiles that account for the stochastic demand generated by the user behavior. The user selects a capacity and its corresponding energy prices in a novel flexible time-and-level-of-use (TLOU) pricing context. This goes beyond a forecasting approach, since it determines how to respond to the expected demand (i.e., the forecast) in a way that ensures user satisfaction, and considers the user cost and the grid requirements.

We propose a two-stage stochastic optimization model that minimizes the cost of booking power capacity and satisfying energy demand. We introduce two approaches to generate the consumption scenarios. In the first approach, we generate the scenarios from the distributions of the start times of the loads. In the second approach, we use a novel algorithm that builds the scenarios from historical consumption data.

The use of capacity profiles offers savings for the users and provides the grid with more information about the operation of the system. One of the main features of this work is that the users do not manage their consumption to follow a fixed cost profile; instead, they can select the electricity prices from a group of tariffs that adjust to their preferences while considering the grid requirements.

This article is structured as follows: the proposed approaches are described in Section 3, the experimental results and analysis are presented in Section 4, and the conclusion is given in Section 5.

3. Proposed Framework

Our framework is based on the concept of a capacity profile. A power capacity profile allows us to establish a trade-off between user energy requirements and peak-oriented grid decisions. The framework uses a two-stage stochastic optimization model to estimate capacity profiles considering the user behavior and a dynamic cost scheme. The consumer books a maximum level of consumption per time frame, providing the grid with information in advance and receiving energy below that level at a discounted price. The utility uses this information for planning purposes and is able to charge a higher price if the user exceeds the specified level.

This paradigm facilitates the integration of renewable resources (which affect the net demand curve and can generate ramping events), and the possibility of providing backup electricity services in a distributed generation context.

A challenge of this type of decision-making is the proper representation of user energy requirements. We represent this demand through consumption scenarios for each time frame. Since this consumption-related information is not always perfect, we propose two approaches, depending on the available information. In the first approach, we build the demand scenarios by aggregating consumption for all the user's activities. These activities or activity-based loads conceptually include any type of appliance or device whose time and frequency of use can be interpreted as a probability distribution. In this case, we assume that we have a complete characterization of these distributions and that the end-user will continue to behave in the same way.

In the second approach, we build the scenarios using a new algorithm that processes recent historical aggregated consumption data. In this case, the optimization problem is solved for the desired time horizon (typically one day) with the updated scenarios provided by the algorithm. This approach is useful when the information available is limited or when the end-users react to prices by modifying their normal consumption patterns and making previous demand knowledge irrelevant. We will come back to this analysis in Section 4.4.

This section continues as follows: the flexible TLOU price structure is introduced in Section 3.1, the stochastic optimization model is presented in Section 3.2, and the two approaches for scenario generation are described in Sections 3.3 and 3.4.

3.1. *Flexible TLOU Price Structure*

Time of use (TOU) pricing is widely implemented for the residential sector. Under TOU the price of energy depends on the time of day. Figure 1 shows the time windows for off-peak, mid-peak, and on-peak tariffs specified by the Independent Electricity System Operator of Ontario (Canada). Each time window is composed of several time frames.

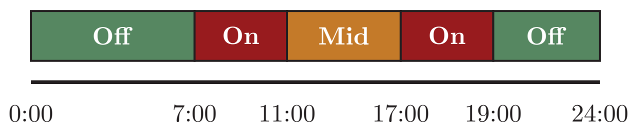

Figure 1: Ontario IESO TOU time windows in winter.

We use a price structure that includes a second dimension: the price also depends on the level of consumption in each time frame. For a specified power capacity, consumption up to this limit is charged at a lower tariff, and consumption above this limit is charged at a higher tariff. This time-and-level-of-use pricing was implemented in [18], where the tariffs and capacity limits were set by the utility or the grid operator. Some pricing strategies that consider power-peak-related penalties are currently available. In Quebec (Canada), the *rate L* for industrial users provides a tariff for the energy consumption, and a tariff for the peak demand [24]. In the case of the residential sector, the national service in Italy supplies electricity up to a maximum constant power limit [25]; no consumption above that limit is allowed.

In the approach presented in this article, the tariff depends on the capacity level booked by the user in each time frame. The utility provides a set of tariffs and capacities from which the consumer can choose. Figure 2 shows the possibilities for the lower tariff; this step function has $| Q^L |$ segments, and the TOU tariff is represented by the parameter K_t^0. Note that all the possible tariffs are $\leq K_t^0$. Selecting $c_t^2 > c_t^1$ allows a cheaper tariff $K_t^{L_2} < K_t^{L_1}$. The higher tariff for consumption above the limit is represented by the function in Figure 3. This step function has $| Q^H |$ segments, and the possible tariffs are $\geq K_t^0$. In this case booking a lower capacity implies a cheaper tariff.

Additionally, we introduce a booking fee K_t^F per power unit that is paid in advance by the user. Determining the

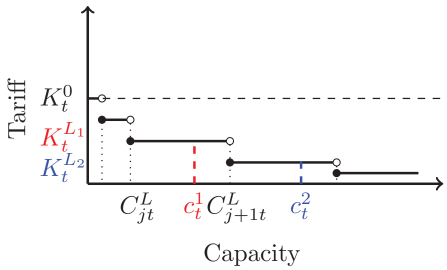

Figure 2: Lower energy tariff as a step function of the booked capacity.

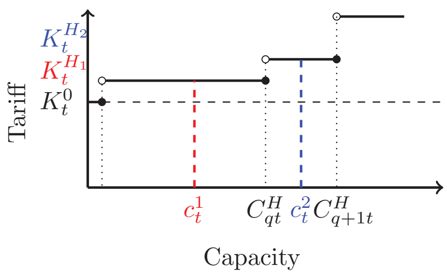

Figure 3: Tariff for consumption above limit as a step function of the booked capacity.

capacity is thus a nontrivial decision. Booking a higher capacity c_t^2 will give a cheaper $K_t^{L_2}$ and a more expensive $K_t^{H_2}$ as well as a higher booking cost $K_t^F c_t^2$.

TLOU offers several features and advantages. First, TLOU proposes a trade-off between the utility and the end-users. The users benefit from cheaper tariffs as long as their consumption is kept under a threshold that each user is able to choose so as to satisfy his demand. The cost associated with these discounted tariffs is paid by the utility, who in return, receives information about the user consumption in order to facilitate system operation.

Second, TLOU offers a form of DSM that is economically beneficial for the utility since it helps to reduce the fluctuation of net demand. Indeed TLOU can eliminate the rebound peaks by promoting a more homogeneous consumption under the selected power capacity regardless the time of the day. In other words, a cost-minimizing user will first consume electricity in the first level of both off-peak and on-peak hours, and only then shift the remaining demand to the second level of an off-peak hour.

Third, with an increasing penetration of distributed generation, TLOU facilitates the integration of new business models in which the users will pay a fixed cost to have the grid connection as a back up for their own local (e.g. solar) generation.

Although there are many potential benefits from a real-world implementation of TLOU, important considerations remain about determining the optimal set of tariffs, depending on the generation technologies, marginal costs, and the consumer acceptance and reaction to this type of program. These aspects are beyond the scope of this article, and are the subject of ongoing research.

3.2. Two-Stage Stochastic Optimization Model

We estimate the capacity by solving a two-stage optimization problem [26]. In the first stage the user determines the capacity required per time frame. The second stage takes into account the cost of meeting the demand and the costs associated with the decision. The objective function (1) includes the booking cost, the expected cost of consumption at the lower tariff, and the expected cost of consumption at the higher tariff.

Constraints (2) and (3) ensure that the booked capacity belongs to one of the intervals of the step functions for both tariffs. Constraints (4) and (5) set the lower and upper bounds for each interval of the step functions. We introduce the auxiliary variable $\bar{c}_{qt}$ for the capacity in the higher-tariff step cost function. Constraint (6) establishes the relationship between the capacity and the auxiliary variable.

Constraints (7) and (8) impose the lower-tariff consumption and the demand satisfaction, respectively, for each scenario. Finally, constraints (9) and (10) are the nonnegativity and binary constraints.

$$\min f = \sum_{t\in T}\sum_{j\in Q^L} K_t^F c_{jt} + \sum_{t\in T}\sum_{j\in Q^L}\sum_{i\in S(t)} \pi_{it} K_{jt}^L x_{ijt}^L + \sum_{t\in T}\sum_{q\in Q^H}\sum_{i\in S(t)} \pi_{it} K_{qt}^H x_{iqt}^H \tag{1}$$

subject to

$$\sum_{j\in Q^L} \phi_{jt} = 1, \quad \forall t\in T \tag{2}$$

$$\sum_{q\in Q^H} \delta_{qt} = 1, \quad \forall t\in T \tag{3}$$

$$\phi_{jt} C_{jt}^L \le c_{jt} \le \phi_{jt} C_{j+1t}^L, \forall j\in Q^L, j <\mid Q^L \mid -1, t\in T \tag{4}$$

$$\delta_{qt} C_{qt}^H \le \bar{c}_{qt} \le \delta_{qt} C_{q+1t}^H, \forall q\in Q^H, q <\mid Q^H \mid -1, t\in T \tag{5}$$

$$\sum_{j\in Q^L} c_{jt} - \sum_{q\in Q^H} \bar{c}_{qt} = 0, \quad \forall t\in T \tag{6}$$

$$x_{ijt}^L \le c_{jt}, \quad \forall i\in S(t), j\in Q^L, t\in T \tag{7}$$

$$\sum_{j\in Q^L} x_{ijt}^L + \sum_{q\in Q^H} x_{iqt}^H \ge D_{it}, \quad \forall i\in S(t), t\in T \tag{8}$$

$$x_{ijt}^L, x_{iqt}^H, c_{jt}, \bar{c}_{qt} \ge 0, \forall i\in S(t), j\in Q^L, q\in Q^H, t\in T \tag{9}$$

$$\phi_{jt}, \delta_{qt} \in \{0,1\} \quad \forall j\in Q^L, q\in Q^H, t\in T \tag{10}$$

In the model the capacity requirements are computed by time frame; in a more realistic scenario the grid operator could assign capacity profiles over a longer horizon of consumption. In the context of TOU we can identify several time windows (groups of time frames) with the same price (for example, off-peak, mid-peak, and on-peak tariffs). Given a set W of time windows, we could enforce the same capacity for the time frames in the same time window by adding constraint (11):

$$c_{jt} = c_{jt'} \quad \forall j \in Q^L, \quad t, t' \in \tau^\omega \mid t \neq t', \quad \omega \in W \qquad (11)$$

where $\tau^\omega \subset T$ is a subset of time frames. This modification to the original model will be explored in Section 4.

3.3. Scenario Generation from Distributions (SfD)

In this section we present the SfD approach to assemble the demand scenarios when we know the individual load distributions. We assume that the start or arrival time of each load follows a normal distribution $X_{mt} \sim \mathcal{N}(\mu_m, \sigma^2)$ [27, 28]. The duration L_m and the level of consumption P_m of each appliance are deterministic parameters.

The aggregation of individual loads can result in numerous scenarios since each time t has $\sum_{m=1}^{|M|} \binom{|M|}{m}$ possible consumption levels obtained from the possible arrivals of the loads. Including zero consumption, we have for each time frame $\sum_{m=1}^{|M|} \binom{|M|}{m} + 1 = \sum_{m=0}^{|M|} \binom{|M|}{m} = 2^{|M|}$ possible consumption levels or scenarios.

The arrival distribution of each load m is discretized over $\mid T \mid$ time frames, and the probability that load m starts in time frame t is denoted $\mathbb{P}(X_{mt} = 1)$.

We also need to consider the load durations, so we define the probability that load m is active in time frame t as:

$$\mathbb{P}(\tilde{X}_{mt} = 1) = \sum_{a=t-L_m}^{t} \mathbb{P}(X_{ma} = 1),$$

which is the accumulated probability over the duration L_m of the load. Finally, we compute the probability that scenario i occurs in time frame t as

$$\pi_{it} = \prod_{m \in i} \mathbb{P}(\tilde{X}_{mt} = 1) \prod_{m \notin i} (1 - \mathbb{P}(\tilde{X}_{mt} = 1)).$$

We determine π_{it} by considering the loads that generate its corresponding consumption level. While a maximum consumption peak scenario requires all the loads to be active, a zero consumption scenario requires none of them to be active. For any other level of consumption it is necessary to have some active and some inactive loads. Depending on the parameters of the distribution and the load durations, some of the scenarios can have near-zero probabilities. We remove the scenarios with a probability $< \rho$, where ρ is a significance threshold defined by the decision-maker. The more concentrated the loads are over a set of time frames, the more scenarios can be discarded from this set. Thus, each time frame t can have a different number of scenarios (i.e., $S(t)$). Finally, the demand D_{it} is computed by adding the individual power consumption P_m of the loads active in each scenario and time frame.

Once we have the parameters D_{it} and π_{it} we solve the optimization model and the solution obtained do remain optimal as long as the user's distributions will not change.

3.4. Scenario Generation from Historical Data (SfH)

The SfH approach presented in this section determines capacity profiles using information about which time frames are more likely to have consumption based on the user's historical demand profiles.

This consumption information is contained in the matrix $\Gamma \in \mathbb{R}^{N \times |T|}$ for a set of N previous days. We use the data in Γ to split the horizon into several segments G and then to allocate a capacity c_t to each time frame. Note that although a segment of time can be composed of several time frames, it does not necessarily match the time windows of the pricing policy.

First, we identify several contiguous submatrices in Γ by clustering time frames based on proximity and consumption. Each submatrix contains either only time frames with no consumption (columns of zeros) or columns with some consumption over the historical set. Equation (12) shows Γ for four days and six time frames; we can identify four segments: columns 1, 2–3, 4–5, and 6.

$$\Gamma = \begin{pmatrix} \mathbf{0} & 0 & \lambda & \mathbf{0} & \mathbf{0} & 0 \\ \mathbf{0} & \zeta & 0 & \mathbf{0} & \mathbf{0} & \lambda \\ \mathbf{0} & 0 & \kappa & \mathbf{0} & \mathbf{0} & 0 \\ \mathbf{0} & 0 & \lambda & \mathbf{0} & \mathbf{0} & 0 \end{pmatrix} \qquad (12)$$

After this identification we discard the time frames where loads are not expected based on the historical data.

Second, we determine π_{it} and D_{it} in Γ by listing demand observations and computing their frequency per column. For example, there are three scenarios in column 3: $D_{1,3} = \lambda$, $D_{2,3} = \kappa$, $D_{3,3} = 0$, with $\pi_{1,3} = 0.5$, $\pi_{2,3} = 0.25$ and $\pi_{3,3} = 0.25$. Finally, we solve the optimization problem.

We must decide the size of N before determining the capacity profile. Too few days (rows) in Γ could result in insufficient information. On the other hand, increasing the number of days may not add significant information or could introduce rare events that do not represent typical user behavior. Experimentally we observe that as the number of days n increases, the number of segments $\bar{G}(n)$ initially increases and then decreases until it reaches a constant value because of the finite horizon. We continue including days and identifying segments until we have added β days without changing the number of segments. Algorithm 1 presents this process in detail.

3.4.1. Algorithm termination

We prove that Algorithm 1 terminates by proving the existence of an upper bound for $\bar{G}(n)$ and monotonically decreasing behavior after this maximum value has been reached.

Let z_t^n be a parameter indicating whether or not column t of matrix Γ at iteration n is an all-zero column:

$$z_t^n = \begin{cases} 1 & \text{If column } t \text{ is zero} \\ 0 & \text{Otherwise} \end{cases}$$

Algorithm 1 Dynamic Capacity profile

Initialization

- $n = 0$ Iteration number (i.e., days added)
- $\alpha = 0$ Number of iterations with the same number of segments

Obtain number of segments

while $\alpha < \beta$ **do**
$n \leftarrow n + 1$
Add a row to Γ
Compute $\bar{G}(n)$ by identifying the number of segments in Γ
if $\bar{G}(n) = \bar{G}(n-1)$ **then**
$\alpha = \alpha + 1$
else
$\alpha = 0$
end if
end while
$N \leftarrow n$
$G \leftarrow \bar{G}(n)$

Compute Scenarios
Determine π_{it} and D_{it} for each column in Γ by listing demand observations and computing their frequency
Solve Optimization Problem (1)–(10)

We can determine the number of segments via:

$$\bar{G}(n) = y(n) + 1$$

where $y(n)$ is the number of transitions between zero and nonzero columns, and $\bar{G}(n)$ is an integer value in the interval $[0, \mid T \mid]$:

$$y(n) = \sum_{t=1}^{|T|-1} (z_t^n - z_{t+1}^n)^2.$$

Lemma 1. *There exists $G^{\max}$ such that $\bar{G}(n) \leq G^{\max}$ for a given horizon $\mid T \mid$.*

Proof. The maximum value for each pair $(z_t^n - z_{t+1}^n)^2 = 1$, so $y^{\max} \leq \mid T \mid -1$ and $G^{\max} \leq \mid T \mid$. Therefore, $G^{\max}$ exists. □

Lemma 2. *After $\bar{G}(n)$ reaches $G^{\max}$, $\bar{G}(n)$ is monotonically decreasing.*

Proof. We know that the number of rows in Γ increases at each iteration, so

$$z_t^{n+1} \geq z_t^n, \quad \forall \quad n = 1 \ldots N, \quad \forall \quad t \in T.$$

If $z_t^{n+1} = z_t^n \quad \forall \quad t \in T$, then $y(n+1) = y(n)$ and $\bar{G}(n+1) = \bar{G}(n)$.

If there exists t such that $z_t^{n+1} > z_t^n$, then there exists a pair $(z_t^n - z_{t+1}^n)^2 = 0$, $y(n+1) \leq y(n) - 1$, and $\bar{G}(n+1) \leq \bar{G}(n) - 1$. □

Theorem 1. *Algorithm 1 terminates.*

Proof. Because $y \geq 0$ and $G \geq 0$, by lemma 2 the algorithm must terminate. □

4. Experimental Results

In this section we report the results from our experiments with the framework presented in Section 3. In Section 4.1 we introduce the instances used, followed in Section 4.2 by a discussion of the results and properties of the optimization model, and in Section 4.3 by a simulation that validates and compares the proposed approaches for scenario generation. Section 4.4 reports the results and analysis for an instance in which the end-user changes the distributions in reaction to the tariffs. The experiments were carried out in Matlab using Cplex 12.7.0 for a single user with multiple activity-based loads.

4.1. Instances

We explore changing the number of loads, the standard deviation of the loads' arrival times, and the concentration of the loads' arrivals (i.e., how close the loads arrive to each other). The first impacts the number of scenarios and the aggregated consumption level; the second and third affect the congestion over a time window. We denote the instances with $\Phi_{|M|\sigma\bar{x}}$ where $\mid M \mid = \{3, 5, 10\}$, $\sigma = \{0.5, 1, 2\}$, and $\bar{x} = \{1\text{: low, } 2\text{: medium, } 3\text{: high}\}$ concentrations of the arrival of the loads over similar time frames. In the experiments the time frames are equivalent to hours. Figure 4 shows the values for $\bar{x}$.

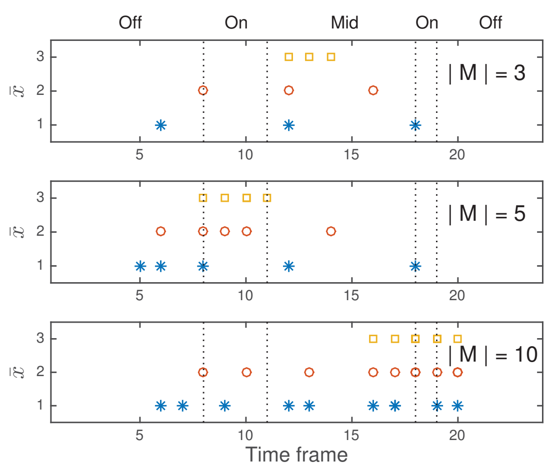

Figure 4: Concentration of load arrivals.

We observe that the activities become closer as $\bar{x}$ increases. They cluster in the mid-peak frames for $\mid M \mid$

$= 3$, in the on-peak frames for $\mid M \mid = 5$, and spread over the evening for $\mid M \mid = 10$.

The load sets are defined as follows: For $\mid M \mid = 3$ $L_m = \{3, 2, 1\}$ and $P_m = \{2.8, 1.8, 0.8\}$. For $\mid M \mid = 5$ we add two more loads with $L_m = \{1, 2\}$ and $P_m = \{0.5, 0.4\}$. Finally for $\mid M \mid = 10$ we add five more loads with $L_m = \{1, 1, 1, 1, 1\}$ and $P_m = \{0.5, 1.0, 1.5, 1.5, 0.5\}$ to the previous sets.

Figure 5 shows the resulting expected consumption profiles. These are computed with the information from Figure 4, combined with each value in σ and taking into account the duration of the loads. The consumption peaks are typically generated when the concentration $\bar{x}$ is high and σ is low. In these cases the higher tariff of the TLOU accounts for the additional costs that the grid incurs to maintain the balance between supply and demand.

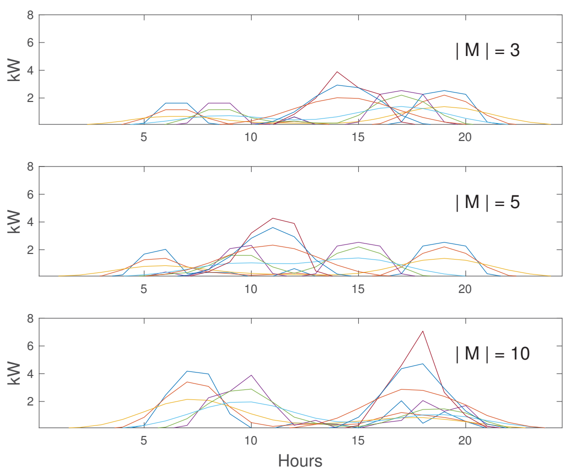

Figure 5: Expected consumption profiles.

4.2. Stochastic Optimization

Table 1 shows the total cost and total capacity c^{tot} over the horizon, obtained by solving two versions of the model presented in Section 3.2: Model 1: Equations (1)–(10) and Model 2: Equations (1)–(11). Both models are solved for all combinations of the parameters previously introduced.

The resulting optimization problems are composed by 216 binary variables, and up to 40,000 continuous variables and 20,000 constraints depending on the number of scenarios $I(t)$.

Let us start with the side of the table that corresponds to Model 1. This model computes a capacity value for each time frame. If we analyze each row (keeping σ and $\bar{x}$ fixed) we see that c^{tot} increases as we introduce more activity-based loads. In fact, there is a strong correlation (about 80%) between the total demand and the total capacity booked.

We see that as σ increases c^{tot} decreases for $|M| = 3$ in the three scenarios of $\bar{x}$. This behavior is different for $|M| = 5$ and $|M| = 10$ where the combination of σ and $\bar{x}$ reports higher total capacities even in cases with higher standard deviation.

At this point we need to consider the interaction of the parameters to understand how the optimization model is working, since they determine the shape of the expected demand curve. Figure 6 show some examples.

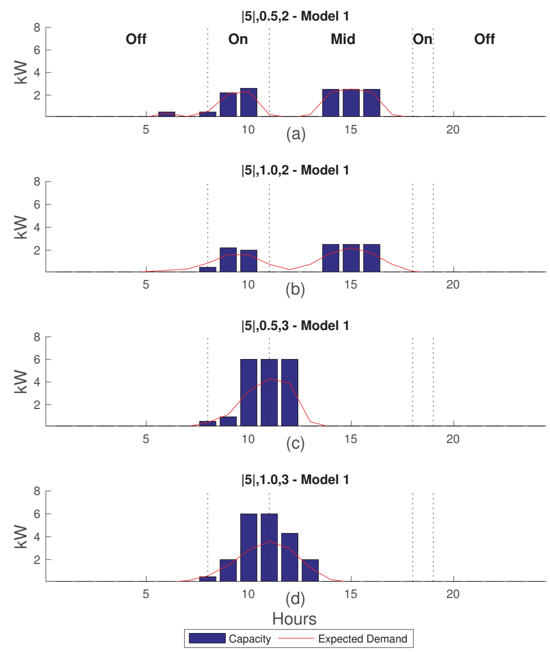

Figure 6: Example of effect of σ and $\bar{x}$ on c^{tot}.

We change σ in Figures 6(a) and 6(b) while keeping the other parameters constant. For $\sigma = 0.5$ we obtain $c^{tot} = 13.3$. A higher $\sigma = 1.0$ flattens the expected demand curve, resulting in a lower $c^{tot} = 12.2$.

Similarly, we change σ in Figures 6(c) and 6(d), this time with $\bar{x} = 3$. In this case $\sigma = 1.0$ results in a higher $c^{max} = 20.8$ compared to $\sigma = 0.5$ with a $c^{max} = 19.4$. Although the demand curve is flattened, it is still high enough to make it economical to buy capacity in advance, due to the proximity of the different loads over time. We can see this clearly at $t = 13$, where the expected demand changes from 0.1 in 6(c) to 1.1 in 6(d).

Now we analyze the columns in Table 1 that correspond to Model 2. This model determines capacity profiles for each time window. We observe that none of the parameters has a clear trend with respect to the total capacity. In this case, we additionally need to consider whether the loads are concentrated over a single time window or not. Figure 7 shows the comparison of Model 1 and Model 2 for two specific instances.

Figures 7(a) and 7(b) present results for the first instance. The hourly capacity (Figure 7(a)) gives a higher c^{tot} than the window-wise capacity from 7(b). The dis-

Table 1: Total cost (¢) and total capacity (kWh) for the instances $\Phi_{|M|\sigma\bar{x}}$

	Model 1						Model 2					
	$\mid M \mid = 3$		$\mid M \mid = 5$		$\mid M \mid = 10$		$\mid M \mid = 3$		$\mid M \mid = 5$		$\mid M \mid = 10$	
	Cost	c^{tot}	Cost	c^{tot}	Cost	c^{tot}	Cost	c^{tot}	Cost	c^{tot}	Cost	c^{tot}
$\Phi_{\|M\|0.5,1}$	142.7	12.3	158.6	13.6	217.8	**23.8**	147.5	5.0	164.3	5.0	242.3	**3.0**
$\Phi_{\|M\|1.0,1}$	147.0	11.5	159.4	11.5	226.3	21.0	149.0	5.0	161.7	5.0	240.5	3.0
$\Phi_{\|M\|2.0,1}$	149.6	7.5	161.6	7.5	232.5	16.0	149.8	5.0	161.8	5.0	236.8	8.0
$\Phi_{\|M\|0.5,2}$	171.2	12.3	181.6	**13.3**	271.8	22.7	186.5	5.0	193.9	**23.0**	276.6	20.0
$\Phi_{\|M\|1.0,2}$	172.1	11.5	184.9	**12.2**	267.5	21.3	179.8	5.0	190.2	23.0	268.6	20.0
$\Phi_{\|M\|2.0,2}$	169.0	7.5	188.2	10.5	255.2	16.5	170.5	0.0	189.4	14.0	256.1	11.0
$\Phi_{\|M\|0.5,3}$	141.8	15.3	190.0	**19.4**	237.3	23.0	149.7	24.0	207.6	16.0	254.7	14.2
$\Phi_{\|M\|1.0,3}$	147.4	14.8	193.3	**20.8**	223.7	24.0	151.6	24.0	204.0	16.0	236.9	12.0
$\Phi_{\|M\|2.0,3}$	161.7	14.5	194.8	16.5	212.2	24.5	162.7	12.0	199.4	16.0	220.2	12.0

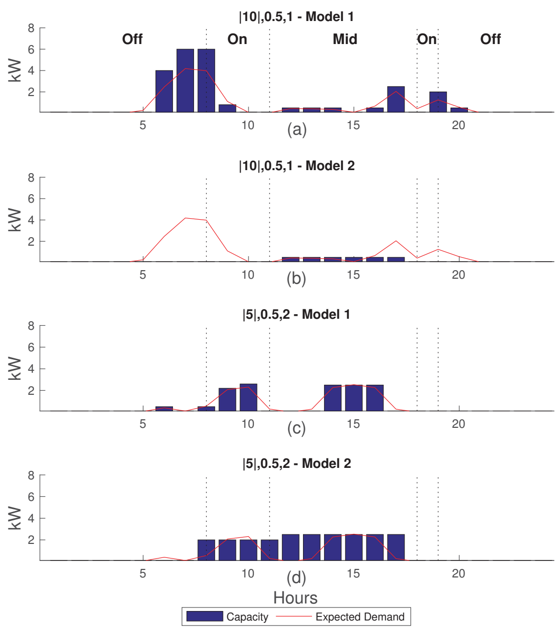

Figure 7: Example of the effect of capacity determination frequency.

persed expected demand makes it inefficient to buy capacity for a full time window.

We observe opposite behavior in Figures 7(c) and 7(d) for the second instance. In this case, the way the expected demand curve fits the defined time windows will give a higher c^{tot} by computing capacity at every time window.

Note that we are analyzing the conditions where the user chooses to buy more or less capacity, and we are not comparing the costs directly since the models are different. In every case, hourly booking is cheaper than booking for a complete window. The latter can be interpreted as a trade-off between simplicity for the utility and savings for the user.

4.2.1. Necessary condition for booking capacity

In Figures 6 and 7 we see that some time frames with an expected demand greater than zero do not have any capacity booked, even in an hourly estimation policy.

We can compare the objective function (1) for a single time frame where it was better not to book instead of booking c (for simplicity we do not include the cost interval subscripts from the step functions and the subscript t):

$$\begin{aligned} K^F 0 + \sum_{i \in S} \pi_i D_i K^0 < \\ K^F c + \sum_{i \in S} \pi_i [x_i^L K^L(c) + x_i^H K^H(c)] \end{aligned} \tag{13}$$

Because $D_i = x_i^L + x_i^H$, we can reorganize inequality (13) as

$$\sum_{i \in S} \pi_i [x_i^L [K^0 - K^L(c)] + x_i^H [K^0 - K^H(c)]] < K^F c, \tag{14}$$

where we find a clear relationship: *the net expected savings must be less than the fixed cost from booking capacity c.* The net expected savings are the savings from the lower tariff and the extra cost of consumption at the higher tariff. The optimization seeks a c that violates the condition in inequality (14). If such a c does not exist, it is optimal to retain the TOU pricing K^0.

Because inequality (14) depends strongly on the tariffs, and the tariffs vary depending on the TOU, we observe different behavior for different time frames. We can see this situation in Figure 6(b), where the user buys capacity at $t = 8$, an on-peak period, and not at $t = 13$, a mid-peak period, despite the similar expected demands.

4.3. Simulation

In this section we implement a 180-day simulation corresponding to the period of the TOU winter tariff in Ontario. We generate each day's consumption randomly given the normal distributions from all the instances introduced in Section 4.2. We compare the average cost of the complete simulation for three different approaches:

- No booking of capacity: The user pays the TOU tariff originally offered by the utility.
- Booking capacity using SfD: The user determines the capacity profile at the beginning of the 180-day period and keeps the profile as optimal policy.
- Booking capacity using SfH: The user determines the capacity profile by solving the optimization problem every day with the scenarios computed as described in Section 3.4.

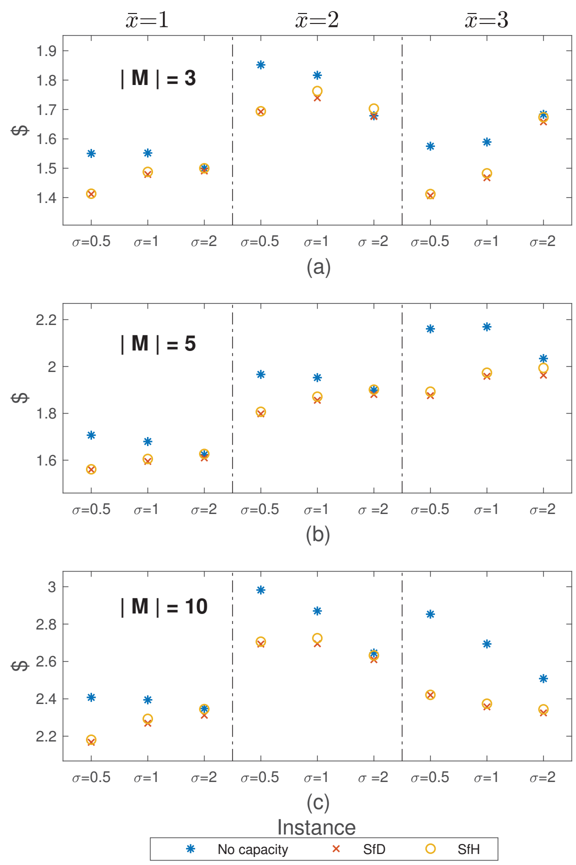

Figure 8: Average cost per day for the instances.

Figure 8 compares the costs of the 27 instances. SfD has the best performance for all the instances since the distributions were known and the user did not change his behavior. SfH represents a trade-off between the potential savings and the available information. It provides optimal values that are close to those of SfD values for all the instances. Finally, the average costs are similar to those in Table 1. In general terms the user achieves savings of up to 16% by participating in TLOU rather than TOU only.

There is a small loss of performance in SfH with respect to SfD that may be interpreted as the value of having perfect information. This gap could be reduced by implementing more sophisticated data analysis approaches that can help to treat the data and achieve a better representation of the user consumption patterns, discarding unnecessary historical observations and predicting in a more accurate way the future user behavior.

We observe some instances where the three approaches report almost the same value. In these cases, the optimization models return a low or zero capacity since the shape of the expected demand curve does not provide significant savings. These instances have the property that the optimal solution is very close to the no-booking policy.

In general, the approaches make a difference when it makes sense to buy capacity in advance. They could be used in combination with a DSM module to create more value for the user.

4.4. User's Reaction to Introduction of TLOU

So far we have assumed that the distributions of the starting times of the loads remained the same during all the simulation. In this section we present some experiments in which the end-user reacts to the introduction of a TLOU program. The user has an initial behavior (i.e. a set of loads' starting time distributions) that changes twice during the simulation. These changes are based on realistic studies presented in [29] and [30] on the consumers reaction to TOU programs offered by utilities. In both cases there is empirical evidence of consumption reduction during peak hours. The effect is stronger during the evening hours (around 15% of reduction) and it is improved by the implementation of smart thermostats that manage the cooling and heating systems, trading off shifting (up to 46% of reduction on peak hours) and user comfort.

We use a 10-load instance for a single user with $L_m = \{1, 2, 1, 1, 2, 1, 1, 1, 2, 2\}$ and $P_m = \{1.5, 1.5, 0.5, 1.0, 0.5, 1.0, 0.5, 0.8, 1.8, 2.5\}$. Figure 9 shows the average consumption profiles of the initial set of distributions (Distr 1) and its two shifting-oriented user reactions (Distr 2 and Distr 3). Observe that the shifting is higher in the on-peak evening hours. Additionally, we reduced the standard deviations for all loads for both distributions sets since the TLOU improves demand predictability ($\sigma^{Distr1} = 1.5$,$\sigma^{Distr2} = 1.0$,$\sigma^{Distr3} = 0.5$.

We carried out simulations for four different cases over 180 days. Distr 1 holds for the first 60 days, Distr 2 for days 61 to 120, and Distr 3 for the last 60 days. In the first case we run a simulation in which the user has a policy of booking no capacity. In the second case we used SfD assuming perfect information. In other words, the stochastic optimization problem is solved at the beginning, and again on days 61 and 121 when the distributions change. We used SfH in the third case . Finally, we include a case where the user solves the stochastic optimization problem at the beginning of the simulation keeping its optimal solution during all the experiment without being aware of the change of distributions (SfD with only the initial distribution). Figure 10 shows the results for these for experiments. We used a moving average filter to facilitate

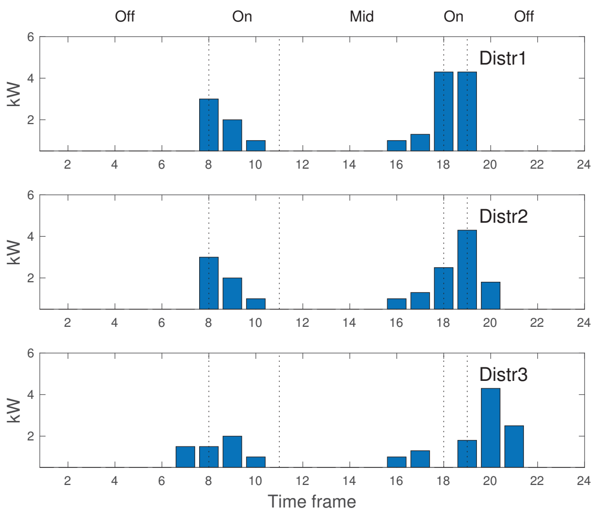

Figure 9: Average consumption profiles for the three sets of distributions.

the data visualization due to the stochastic nature of the problem.

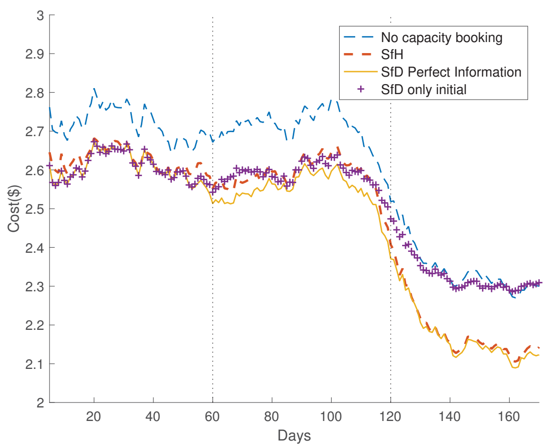

Figure 10: Cost evolution for the four cases.

We can see that in the four cases there is a cost reduction over time; this is due to the shifting from on-peak to off-peak periods. The SfD perfect information case always reports the lowest cost. The SfH approach is able to capture the change in the distributions, achieving a performance close to that of the perfect information case. Finally, we see in the case of SfD with only the initial distributions, that the optimal solution no longer generates savings due to the change in the distributions. This situation is obvious around day 160 where this approach performs worse than the no-booking policy.

5. Conclusion

We have proposed a new framework that allows end-users to profit from a novel flexible TLOU tariff in a DR context.

We formulated a two-stage stochastic optimization model that minimizes the cost of booking power capacity and satisfying energy demand. We introduced two approaches to build the consumption scenarios. In the first approach, we use the distributions of the start time of the loads. In the second approach, we proposed a new algorithm that uses the available historical data.

The use of capacity profiles contributes to the expansion of DR in the residential and commercial sectors, allowing consumers to take advantage of lower prices and providing utilities with a tool that helps to compensate for the extra cost of matching generation and demand in congestion events.

We have provided several scenarios and instances to validate the ideas underlying our approaches. An important aspect of this work is that we consider the user perspective, ensuring satisfaction and obtaining benefits in all the instances. The users are not forced to change their preferences and always satisfy their energy requirements. The experimental results provide insight into how consumers can modify their expected demand curves to gain greater benefits.

Acknowledgments

This research was supported by the Canada Research Chair on Discrete Nonlinear Optimization in Engineering, by the NSERC Energy Storage Technology Network, and by the NSERC-Hydro-Quebec-Schneider Electric Industrial Research Chair on Optimization for Smart Grids.

References

[1] S. Parhizi, H. Lotfi, A. Khodaei, and S. Bahramirad, "State of the art in research on microgrids: A review," *IEEE Access*, vol. 3, pp. 890–925, 2015.

[2] D. Kathan, R. Aldina, M. P. Lee, L. Medearis, P. Sporborg, M. Tita, D. Wight, and W. A., "Assessment of Demand Response and Advanced Metering," *Department of Energy, Washington, DC*, 2012.

[3] P. Siano, "Demand response and smart grids: A survey," *Renewable and Sustainable Energy Reviews*, vol. 30, pp. 461–478, 2014.

[4] L. G. Swan and V. I. Ugursal, "Modeling of end-use energy consumption in the residential sector: A review of modeling techniques," *Renewable and Sustainable Energy Reviews*, vol. 13, no. 8, pp. 1819–1835, 2009.

[5] I. Richardson, M. Thomson, D. Infield, and C. Clifford, "Domestic electricity use: A high-resolution energy demand model," *Energy and Buildings*, vol. 42, no. 10, pp. 1878–1887, 2010.

[6] A. J. Collin, G. Tsagarakis, A. E. Kiprakis, and S. McLaughlin, "Development of low-voltage load models for the residential load sector," *IEEE Transactions on Power Systems*, vol. 29, pp. 2180–2188, Sept 2014.

[7] R. Subbiah, K. Lum, A. Marathe, and M. Marathe, "Activity based energy demand modeling for residential buildings," in *Innovative Smart Grid Technologies (ISGT), 2013 IEEE PES*, pp. 1–6, Feb 2013.

[8] A. Soares, A. Gomes, and C. H. Antunes, "Categorization of residential electricity consumption as a basis for the assessment of the impacts of demand response actions," *Renewable and Sustainable Energy Reviews*, vol. 30, pp. 490–503, 2014.

[9] J. Munkhammar, J. Ryden, and J. Widen, "Characterizing probability density distributions for household electricity load profiles from high-resolution electricity use data," *Applied Energy*, vol. 135, pp. 382–390, 2014.

[10] T. A. Nguyen and M. Aiello, "Energy intelligent buildings based on user activity: A survey," *Energy and Buildings*, vol. 56, pp. 244–257, 2013.

[11] B. P. Esther and K. S. Kumar, "A survey on residential demand side management architecture, approaches, optimization models and methods," *Renewable and Sustainable Energy Reviews*, vol. 59, pp. 342–351, 2016.

[12] F. Fernandes, H. Morais, Z. Vale, and C. Ramos, "Dynamic load management in a smart home to participate in demand response events," *Energy and Buildings*, vol. 82, pp. 592–606, 2014.

[13] Z. Chen, L. Wu, and Y. Fu, "Real-time price-based demand response management for residential appliances via stochastic optimization and robust optimization," *IEEE Transactions on Smart Grid*, vol. 3, pp. 1822–1831, Dec 2012.

[14] J. A. Gomez and M. F. Anjos, "Power capacity profile estimation for building heating and cooling in demand-side management," *Applied Energy*, vol. 191, pp. 492–501, 2017.

[15] M. Rastegar, M. Fotuhi-Firuzabad, and H. Zareipour, "Home energy management incorporating operational priority of appliances," *International Journal of Electrical Power & Energy Systems*, vol. 74, pp. 286–292, 2016.

[16] S. Moon and J.-W. Lee, "Multi-residential demand response scheduling with multi-class appliances in smart grid," *IEEE Transactions on Smart Grid*, 2016.

[17] C. D. Korkas, S. Baldi, I. Michailidis, and E. B. Kosmatopoulos, "Occupancy-based demand response and thermal comfort optimization in microgrids with renewable energy sources and energy storage," *Applied Energy*, vol. 163, pp. 93–104, 2016.

[18] J. A. Gomez and M. F. Anjos, "Collaborative demand-response planner for smart buildings," *Les Cahiers du Gerad*, March 2017.

[19] M. Muratori and G. Rizzoni, "Residential demand response: Dynamic energy management and time-varying electricity pricing," *IEEE Transactions on Power Systems*, vol. 31, pp. 1108–1117, March 2016.

[20] J. S. Vardakas, N. Zorba, and C. V. Verikoukis, "A survey on demand response programs in smart grids: Pricing methods and optimization algorithms," *IEEE Communications Surveys Tutorials*, vol. 17, no. 1, pp. 152–178, 2015.

[21] A. Al Hasib, N. Nikitin, and L. Natvig, "Cost-comfort balancing in a smart residential building with bidirectional energy trading," in *Sustainable Internet and ICT for Sustainability (SustainIT), 2015*, pp. 1–6, IEEE, 2015.

[22] S. Borenstein, "Private net benefits of residential solar pv: The role of electricity tariffs, tax incentives, and rebates," *Journal of the Association of Environmental and Resource Economists*, vol. 4, no. S1, pp. S85–S122, 2017.

[23] S. Afsar, L. Brotcorne, P. Marcotte, and G. Savard, "Achieving an optimal trade-off between revenue and energy peak within a smart grid environment," *Renewable Energy*, vol. 91, pp. 293–301, 2016.

[24] Hydro Quebec, *Electricity rates Effective April 1, 2017*, April 2017.

[25] Servizio Elettrico Nazionale, *Condizioni di fornitura*, 2017.

[26] J. R. Birge and F. Louveaux, *Introduction to Stochastic Programming*. Springer Science & Business Media, 2011.

[27] P. Huppertz, L. Kopczynski, R. Zeise, and M. Kizilcay, "Approaching the diversity of unbalanced residential load in low-voltage grids by probabilistic load-flow simulation of cross-sectional data," in *PowerTech, 2015 IEEE Eindhoven*, pp. 1–6, IEEE, 2015.

[28] J. Dickert and P. Schegner, "A time series probabilistic synthetic load curve model for residential customers," in *PowerTech, 2011 IEEE Trondheim*, pp. 1–6, IEEE, 2011.

[29] M. Harding and C. Lamarche, "Empowering consumers through data and smart technology: experimental evidence on the consequences of time-of-use electricity pricing policies," *Journal of Policy Analysis and Management*, vol. 35, no. 4, pp. 906–931, 2016.

[30] V. Di Cosmo, S. Lyons, and A. Nolan, "Estimating the impact of time-of-use pricing on irish electricity demand," *The Energy Journal*, pp. 117–136, 2014.